Neutrinoless double-beta decay experiments

KamLAND-Zen and future detectors

Nikhef | UNIVERSITY OF AMSTERDAM

Observation of $0\nu\beta\beta$ to confirm neutrinos majorana nature

$2\nu\beta\beta$: $(A, Z) \rightarrow (A, Z+2) + 2e^- + 2\overline{\nu}_e$ $\quad$ $0\nu\beta\beta$ $\quad$ $(T^{0\nu}_{1/2})^{-1} \propto \langle m_{\beta\beta} \rangle^2$

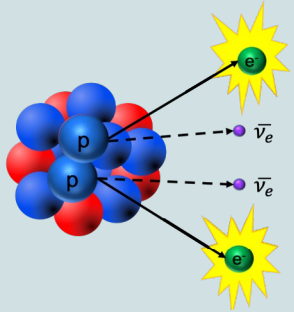

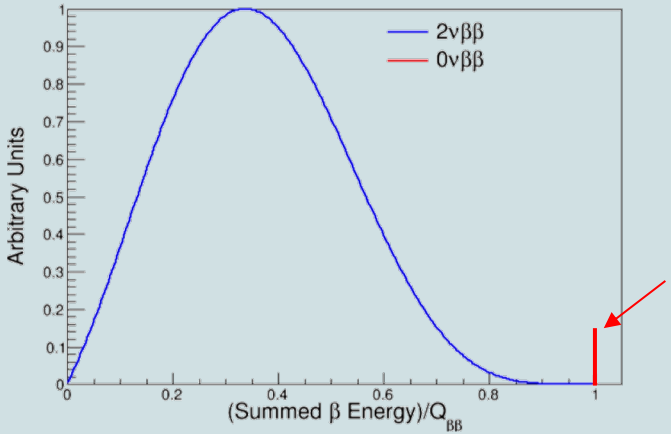

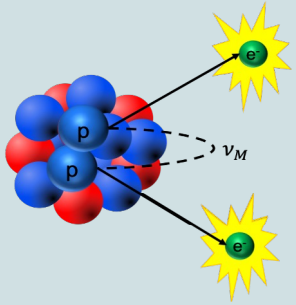

$2\nu\beta\beta$ exceptionally slow nuclear process, $T_{1/2} \sim 10^{19\text{-}21}$ years, so how do we detect $0\nu\beta\beta$?

Experimental design criteria for $0\nu\beta\beta$

Direct searches: kinematic parameters of the two electrons

➔ Total energy and individual electron paths

$$T^{0\nu}_{1/2} = \ln 2 \frac{N_A}{W} \left(\frac{a \cdot \epsilon \cdot M}{N_{\text{obs}}} \right) t \quad \propto \quad a\epsilon \sqrt{\frac{Mt}{N_{\text{bkg}} \cdot \Delta E}}$$

Detector and isotope choice depending on:

- High isotopic abundance — a
- Deployment in large quantity — M
- High-E resolution detector — ΔE
- Low-background conditions — N_{bkg}

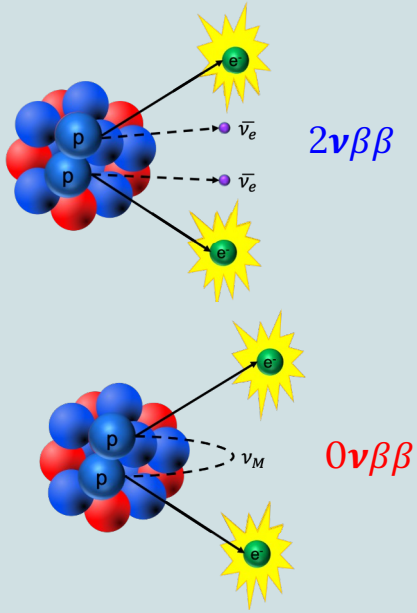

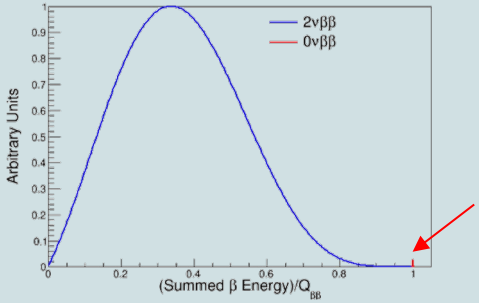

Experimental design criteria for $0\nu\beta\beta$

There are 35 isotopes capable of $\beta\beta$ decay, but not all suitable

Isotope	a (%)	$Q_{\beta\beta}$ (MeV)
^{48}Ca	0.187	4.263
^{76}Ge	7.8	2.039
^{82}Se	8.7	2.998
^{130}Te	34.08	2.527
^{136}Xe	8.9	2.459

$Q_{\beta\beta}$ influence on:

Background

Energy resolution

$$^{136}_{54}\mathrm{Xe} \rightarrow {}^{136}_{56}\mathrm{Ba} + 2e^-$$

$$T^{0\nu}_{1/2} \propto a\epsilon\sqrt{\frac{Mt}{N_{\mathrm{bkg}} \cdot \Delta E}}$$

→ Isotopic abundance

→ Quantity

→ Energy resolution

→ Backgrounds

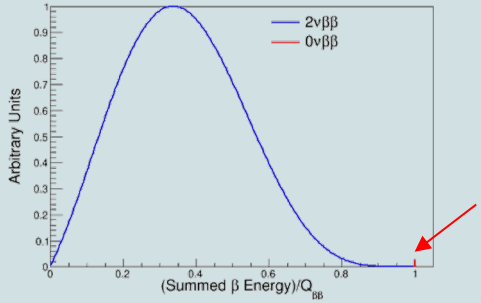

High-sensitive low-background detector necessary.

World-leading experiment: KamLAND-Zen!

KamLAND Collaboration

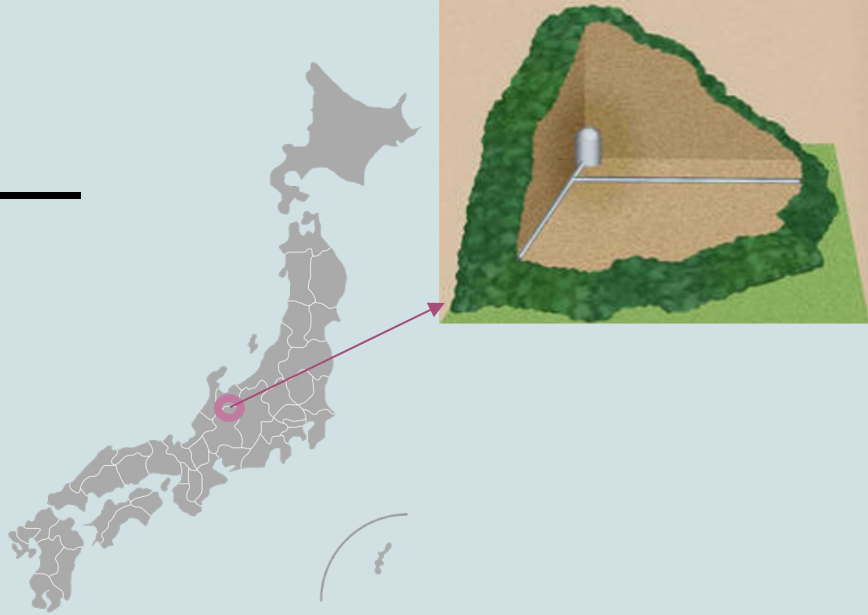

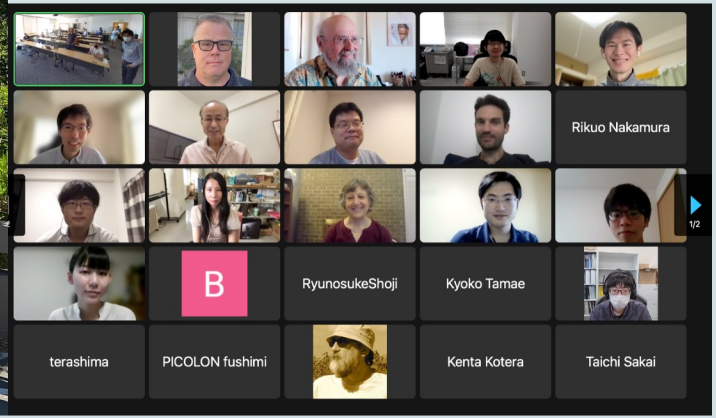

General purpose detector

Solar neutrinos

Geo and reactor neutrinos

Accelerator neutrinos

Astrophysical neutrinos

Neutrinoless double beta decay

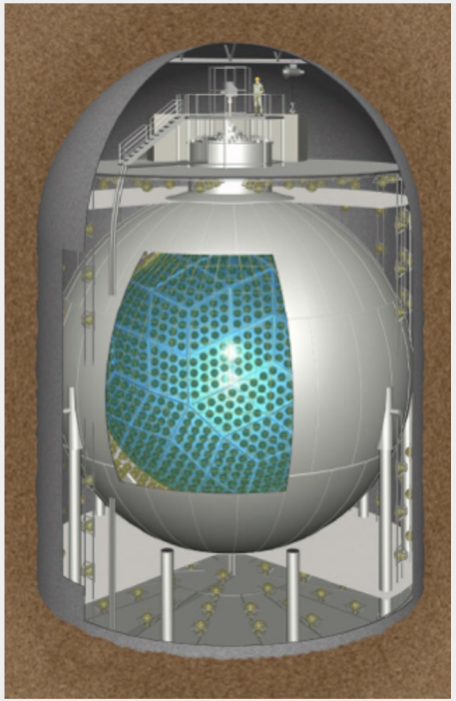

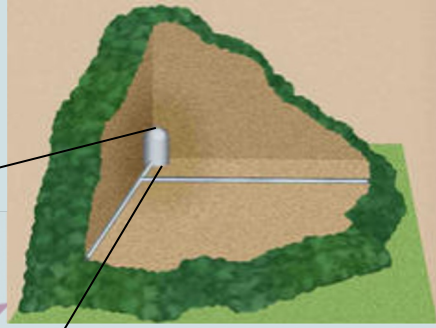

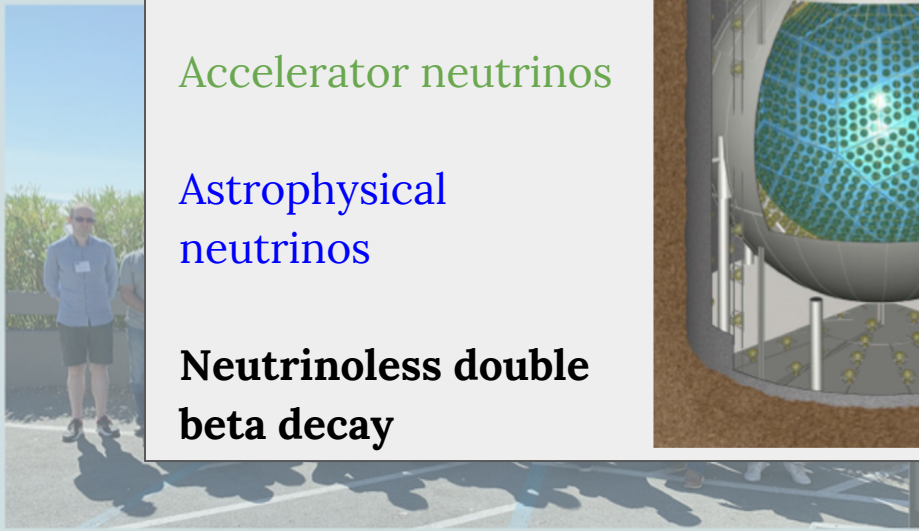

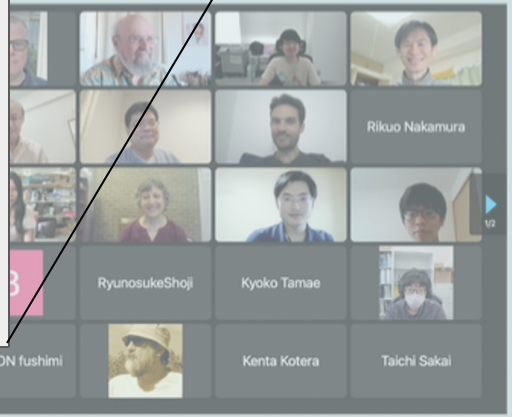

Kamioka Liquid Scintillator Antineutrino Detector

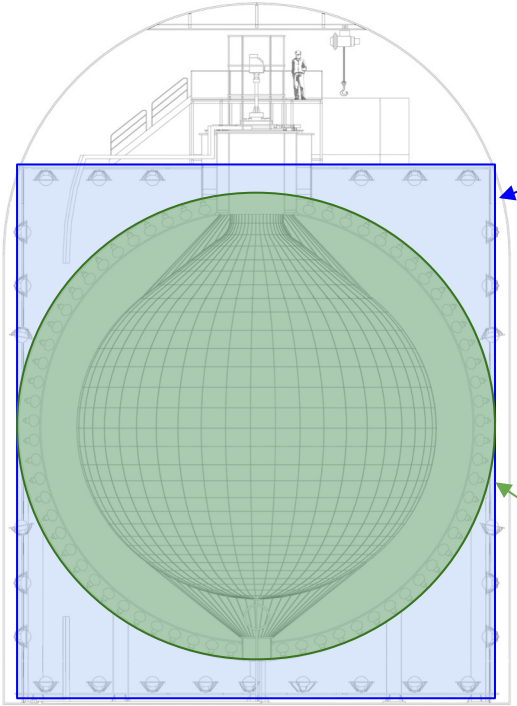

Outer Cherenkov detector

Inner Scintillation detector

Spherical tank, ⌀18m

- 3.2kt pure water

Kamioka Liquid Scintillator Antineutrino Detector

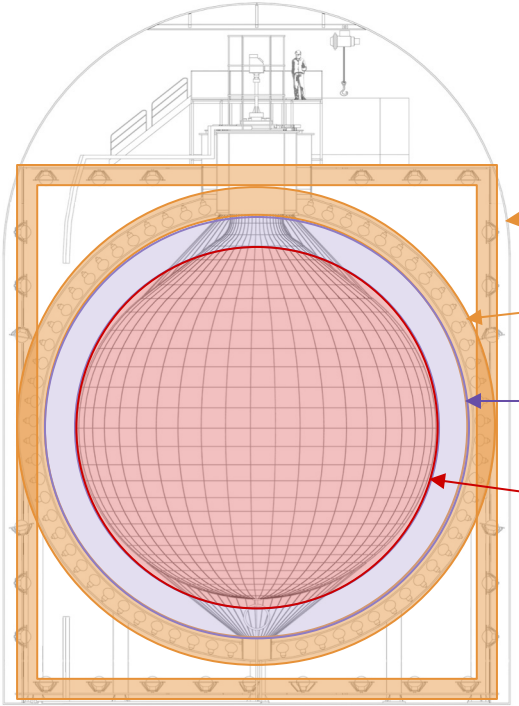

Outer Cherenkov detector

Outer PMTs

Inner PMTs

Buffer oil

Liquid Scintillator balloon

Inner Scintillation detector

Spherical tank, ⌀18m

- 3.2kt pure water

~1800 17- & 20-inch PMTs

Non-scintillation oil 1.8m

KamLAND-LS, ⌀13m, 1.2kt

- Dodecane 80.2%
- Pseudocumene 19.8%
- PPO 1.36g/L

Kamioka Liquid Scintillator Antineutrino Detector

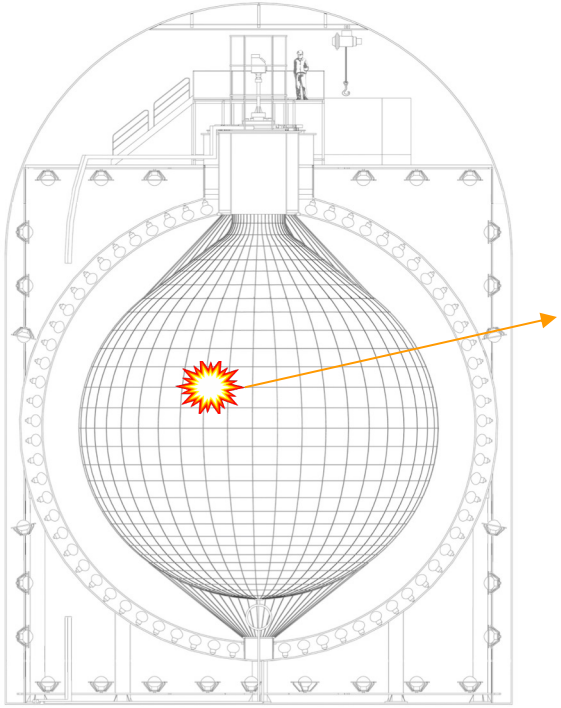

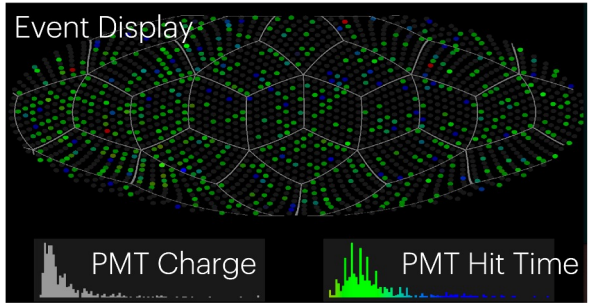

Charge & Timing

↓

Energy & Vertex

Inner detector

- ~ 1300 17-inch PMTs
- ~ 550 20-inch PMTs

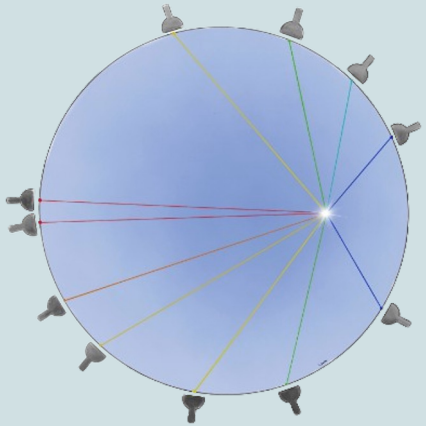

KamLAND-Zen: Zero Neutrino Double Beta

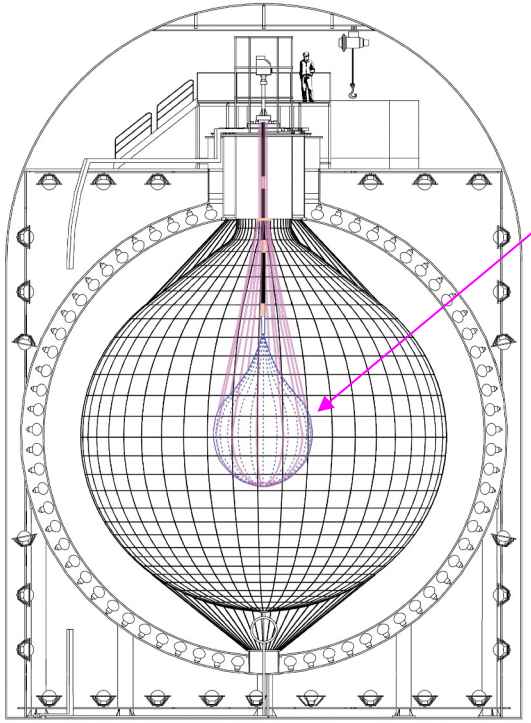

Inner Balloon Xe-LS

$$^{136}_{54}\mathrm{Xe} \rightarrow {}^{136}_{56}\mathrm{Ba} + 2e^-$$

Xe-LS balloon, ⌀3.8m, 24t

- 3.13% enriched xenon

➔ 745 kg ^{136}Xe

➔ 970 kg yr Exposure

$Q_{\beta\beta}$ = 2.458 MeV

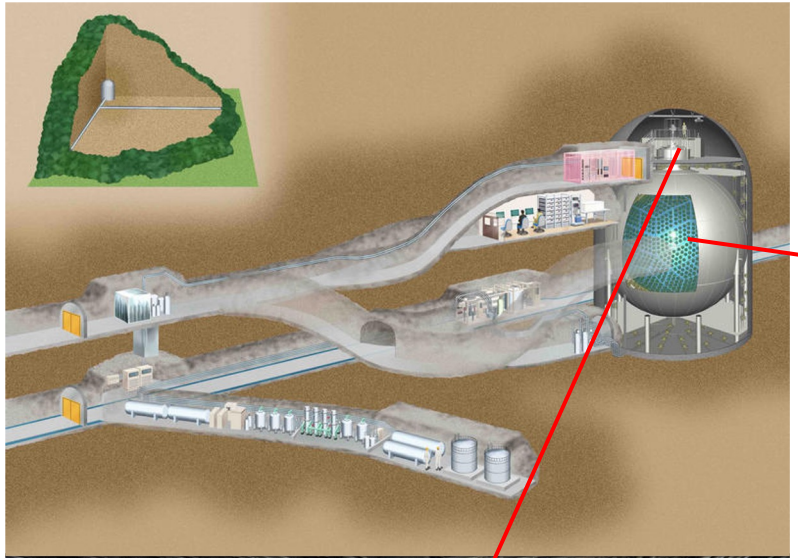

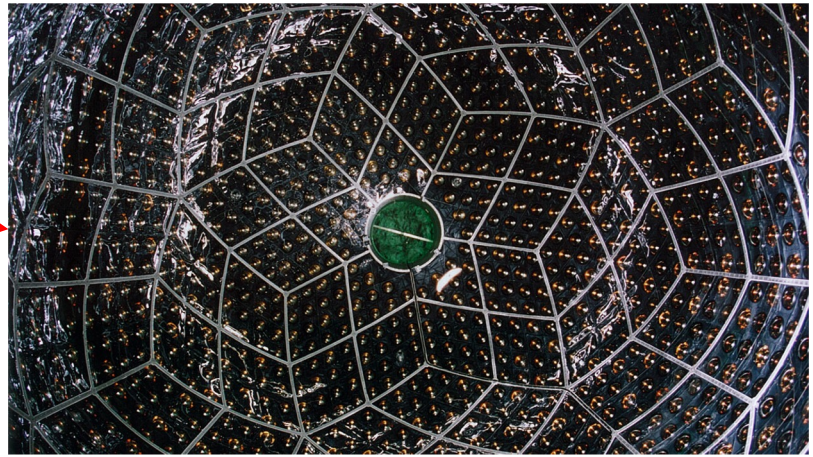

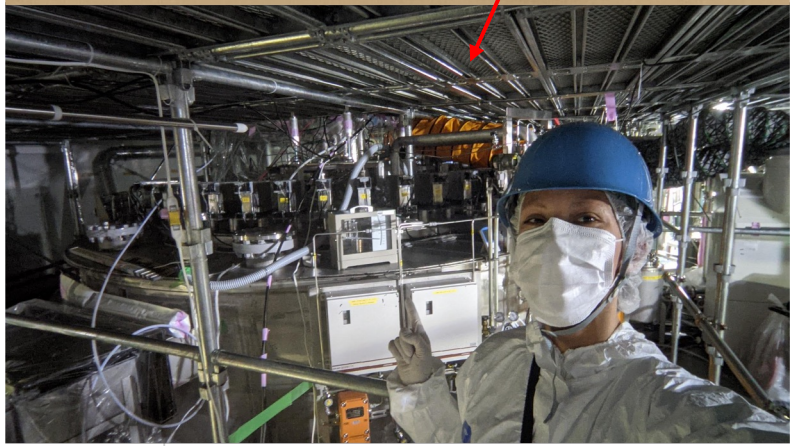

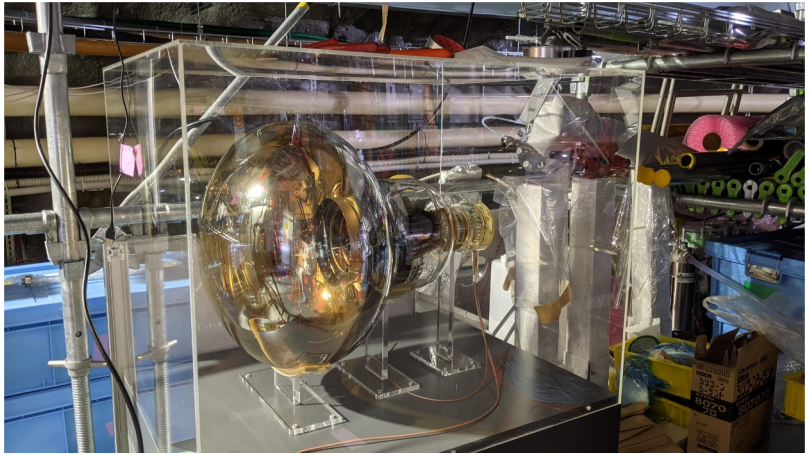

Primary backgrounds and analysis cuts

- $2\nu\beta\beta$ decay
- Cosmogenic spallation products
  - Short-lived: triple coincidence tagging
  - Long-lived: problem
- Solar neutrino interactions
- Radioactive contamination

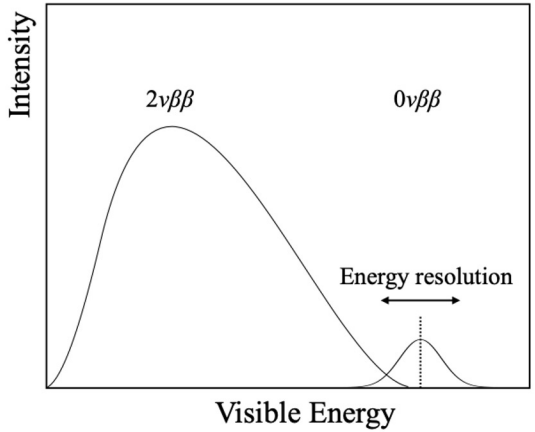

Primary backgrounds and analysis cuts

- $2\nu\beta\beta$ decay
- Cosmogenic spallation products
  - Short-lived: triple coincidence tagging
  - Long-lived: problem
- Solar neutrino interactions
- Radioactive contamination

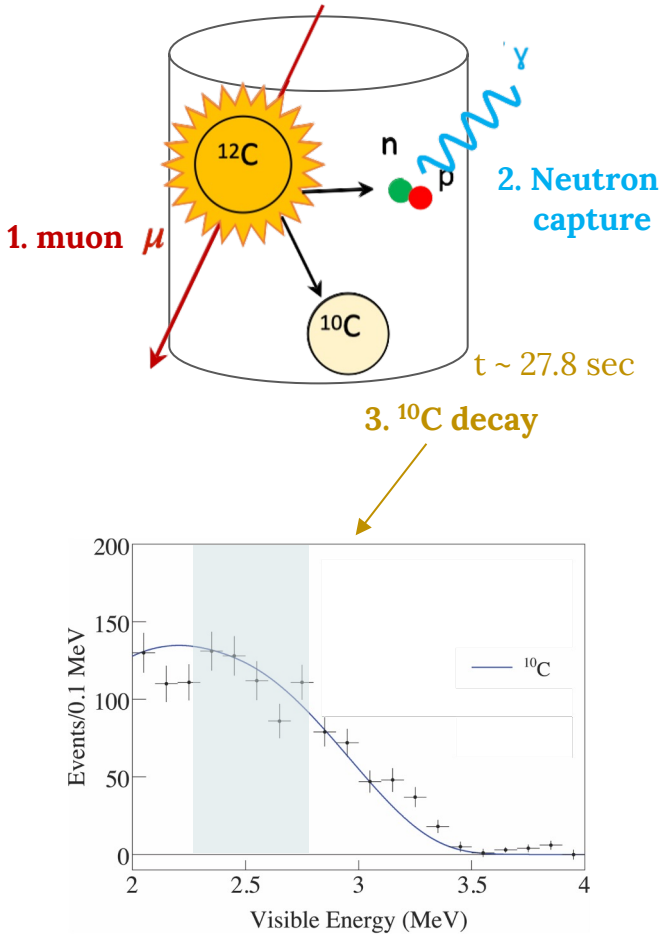

Abe, S., et al. Physical Review C 81.2 (2010): 025807.

Long-lived isotope production from xenon spallation

- Muon spallation on xenon results in long-lived isotopes $T_{1/2}$ ~ (sec - months)

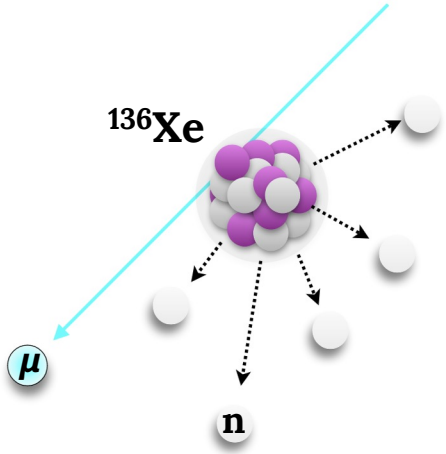

Abe, S., et al. Physical Review C 107.5 (2023): 054612.

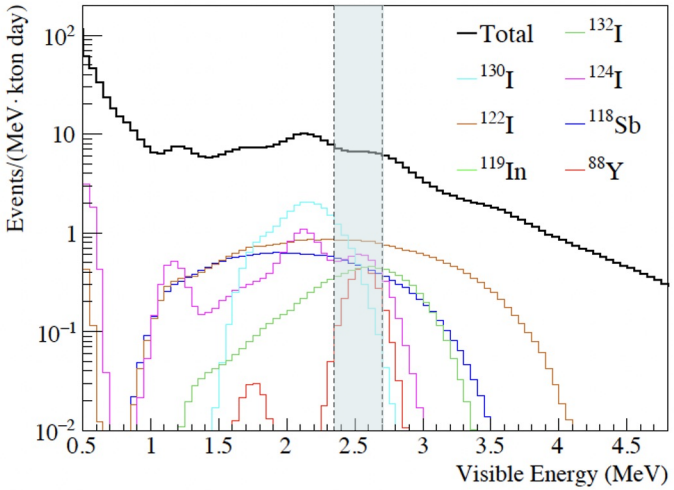

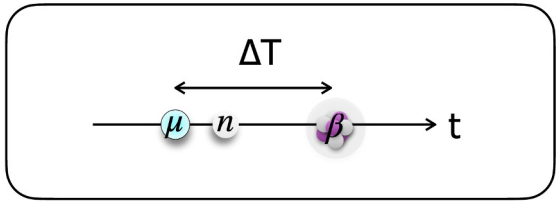

Simulation of spallation products necessary to find correlations

Primary backgrounds and analysis cuts

- $2\nu\beta\beta$ decay
- Cosmogenic spallation products
  - Short-lived: triple coincidence tagging
  - Long-lived: problem
- Solar neutrino interactions
- Radioactive contamination
  - **In** Xe-LS
  - **External** to Xe-LS: IB material

Primary backgrounds and analysis cuts

- $2\nu\beta\beta$ decay
- Cosmogenic spallation products
  - Short-lived: triple coincidence tagging
  - Long-lived: problem
- Solar neutrino interactions
- Radioactive contamination
  - **In** Xe-LS
  - **External** to Xe-LS: IB material

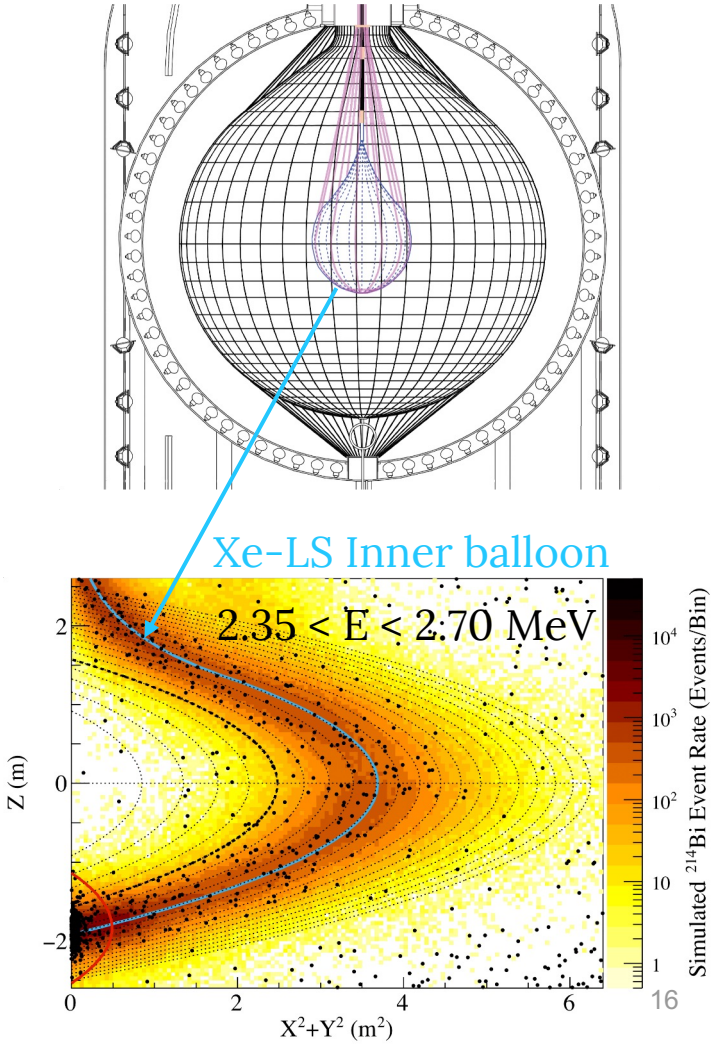

Nikhef | UNIVERSITY OF AMSTERDAM

Primary backgrounds and analysis cuts

- $2\nu\beta\beta$ decay
- Cosmogenic spallation products
  - Short-lived: triple coincidence tagging
  - Long-lived: problem
- Solar neutrino interactions
- Radioactive contamination
  - **In** Xe-LS
  - **External** to Xe-LS: IB material

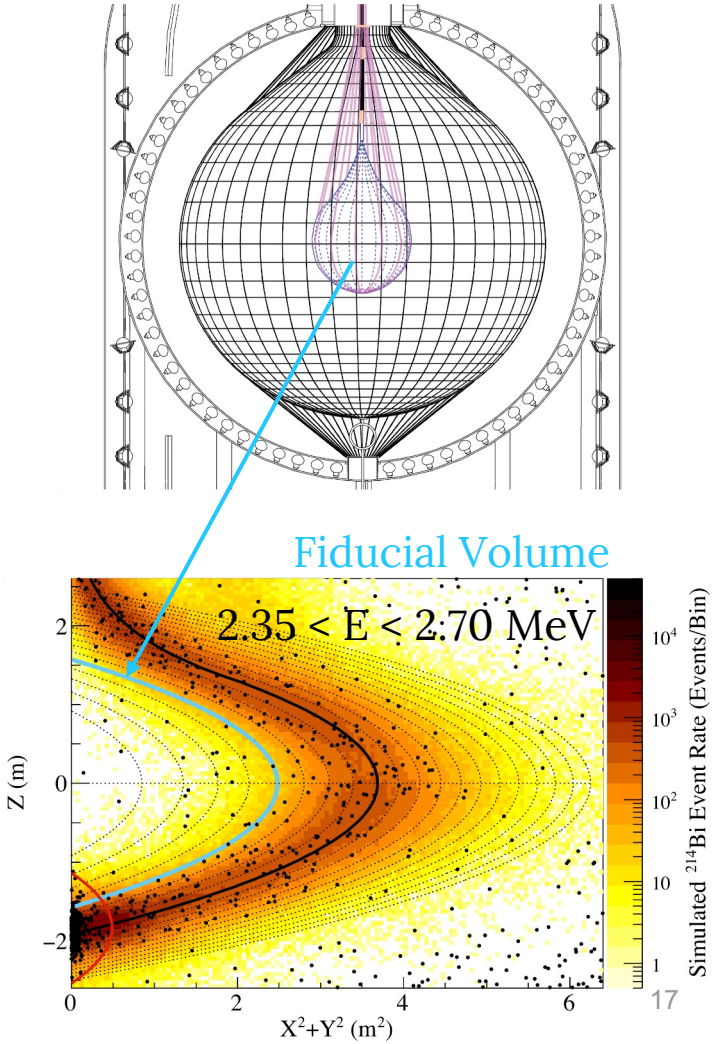

Most stringent limit on the half-life of $0\nu\beta\beta$

Zen Collaboration. (2022). First Search for the Majorana Nature of Neutrinos in the Inverted Mass Ordering Region with KamLAND-Zen. *arXiv preprint arXiv:2203.02139.*

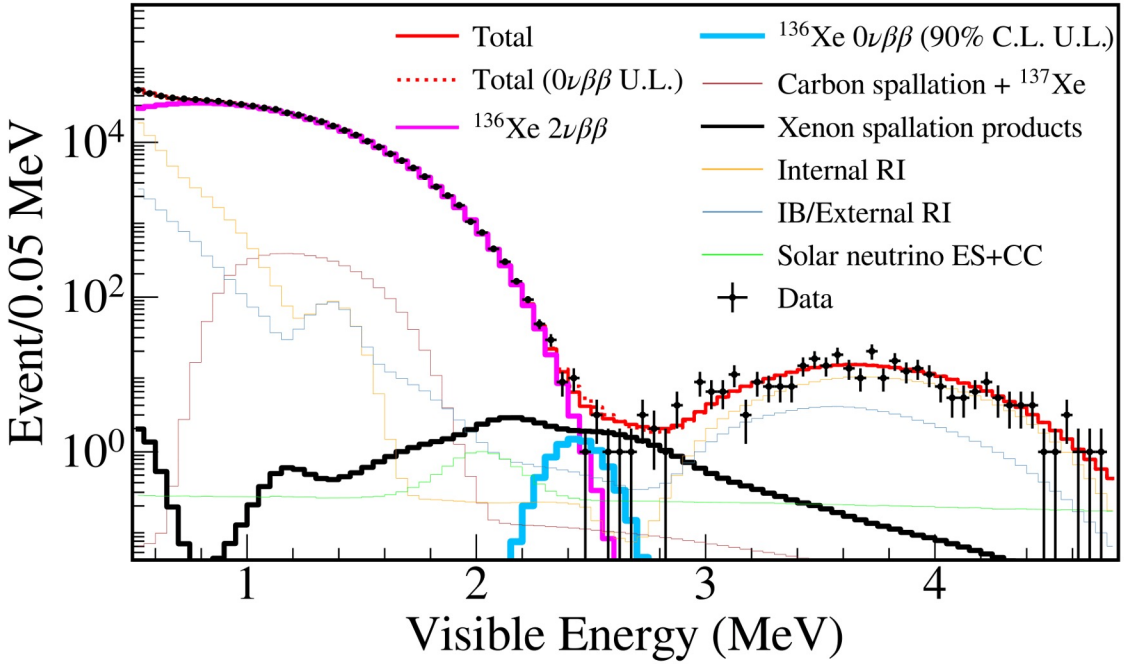

$Q_{\beta\beta}$ = 2.458 MeV

Energy resolution

$$\sim \frac{6.7\%}{\sqrt{E(MeV)}}$$

$$T^{0\nu}_{1/2} > 2.3 \times 10^{26}\ \text{yr}$$

First test of the Majorana nature in the IO region

$$(T^{0\nu}_{1/2})^{-1} = G_{0\nu}(Q,Z)\boxed{|M_{0\nu}|^2}\langle m_{\beta\beta}\rangle^2 \longrightarrow \langle m_{\beta\beta}\rangle = \left|\sum_{i=1}^{3} U_{ei}^2 m_i\right|$$

Nuclear Matrix Element

$$T^{0\nu}_{1/2} > 2.3 \times 10^{26}\ \mathrm{yr}$$

$$\langle m_{\beta\beta}\rangle < (36 - 156)\mathrm{meV}$$

$$m_{\nu 1} > m_{\nu 3}$$

$$m_{\nu 3} > m_{\nu 1}$$

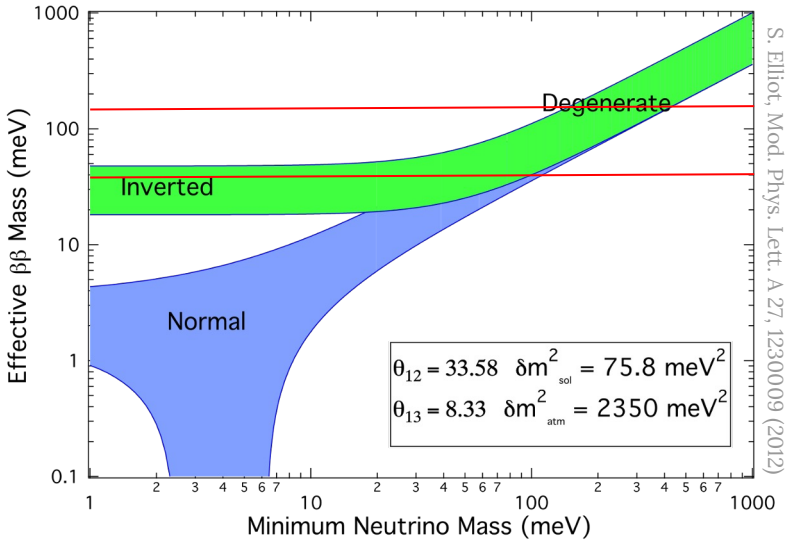

S. Elliot, Mod. Phys. Lett. A 27, 1230009 (2012)

Towards the bottom of the IO region

Most promising isotope candidates: ^{76}Ge | ^{82}Se | ^{100}Mo | ^{130}Te | ^{136}Xe

Leading next-generation ton-scale experiments:

- **CUPID** ^{100}Mo bolometer ← upgrade of CUORE ^{130}Te Bolometer
- **nEXO 5 ton** ^{136}Xe TPC ← upgrade of EXO-200 200kg ^{136}Xe TPC
- **LEGEND-1000** 1 ton ^{76}Ge ← upgrade of LEGEND-200 ^{76}Ge semiconductor

Started data taking very recently

Towards the bottom of the IO region

Agostini, Matteo, et al. Rev. Mod. Phys. 95, 025002 (2023)

^{100}Mo | ^{130}Te | ^{82}Se | ^{136}Xe |

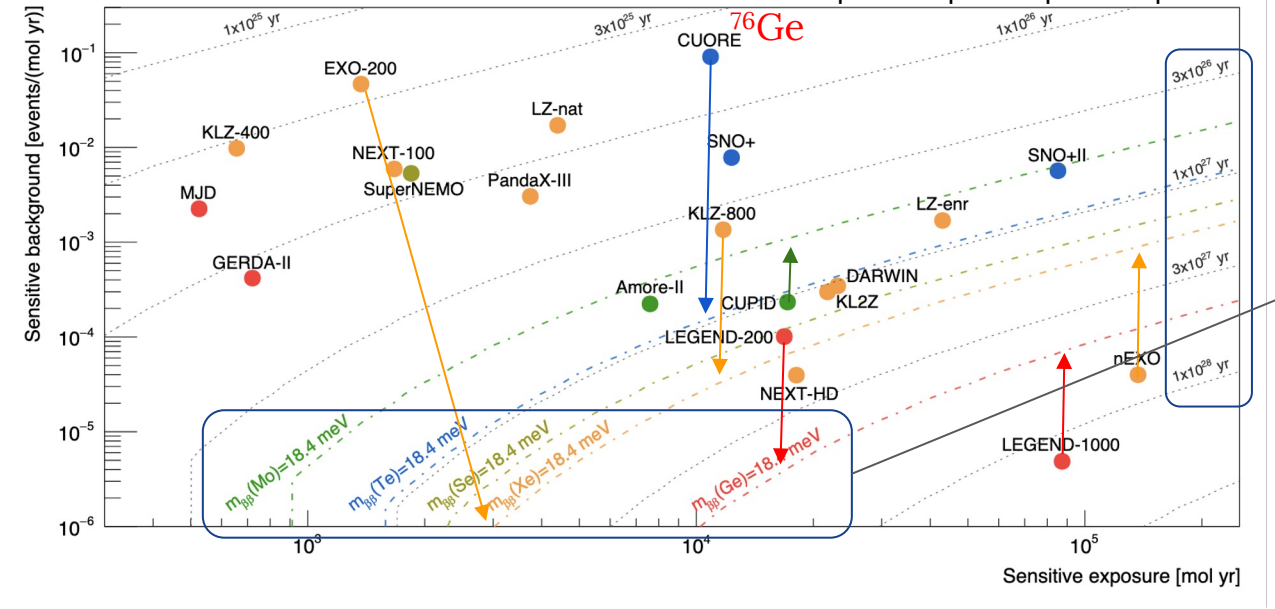

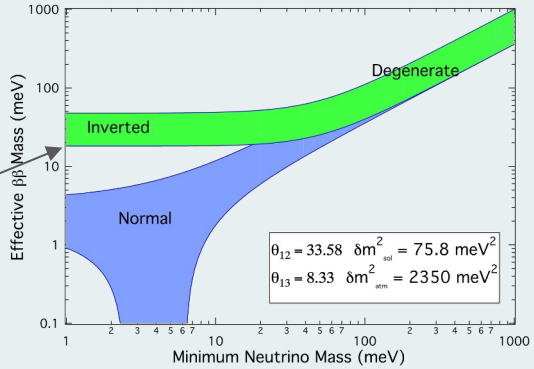

XENONnT + LUX-ZEPLIN + DARWIN = XLZD

ab initio data from PC A. Belley

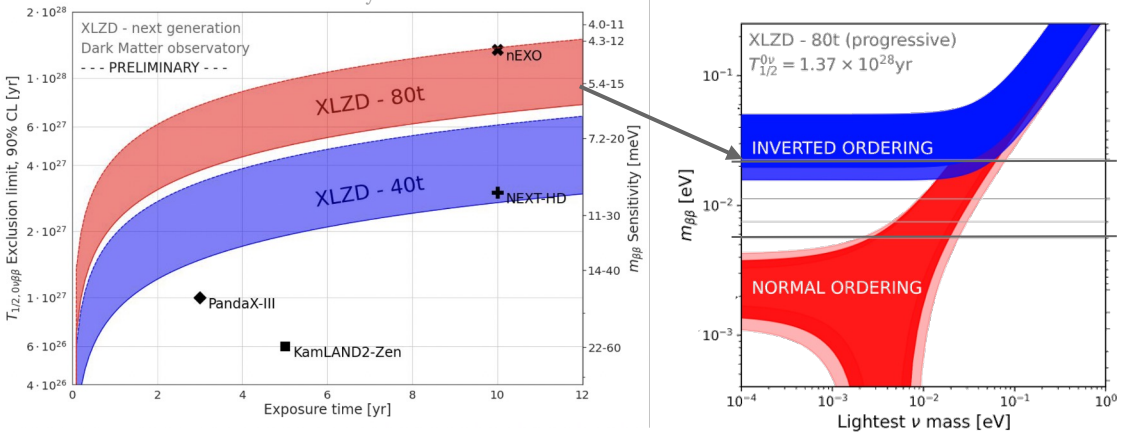

Future DM detector possibly functioning as high sensitive $0\nu\beta\beta$ experiment

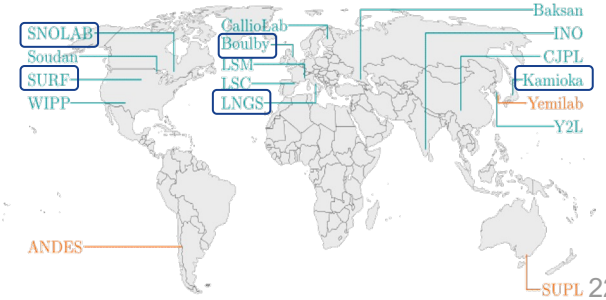

Future perspectives

- ➢ Current most stringent limit is at $T_{1/2} > 2.3 \times 10^{26}$ yr → $m_{\beta\beta} < (36 - 156)$meV

Next-generation detectors reach the bottom of IO and a significant part of NO

- ➢ LEGEND-1000, nEXO and XLZD explore the NO

✓ $0\nu\beta\beta$ is discovered in the IO region → identify LNV physics

✗ $0\nu\beta\beta$ is not discovered in IO region → increase scale and sensitivity of experiments

! Next-next-generation experiments ready by time ton-scale experiments complete !

Thank you for your attention!

Backup slides

KamLAND-Zen upgrade

- **KamLAND2-Zen**
  - 1000 kg enriched Xenon
  - Improved energy resolution: $2\nu\beta\beta$ background reduced
  - Scintillating inner balloon

$$T^{0\nu}_{1/2} > 2.3 \times 10^{26}\ \mathrm{yr} \longrightarrow T^{0\nu}_{1/2} > 2 \times 10^{27}\mathrm{yr}$$

$$\langle m_{\beta\beta} \rangle \sim (36 - 156)\ \mathrm{meV} \longrightarrow \langle m_{\beta\beta} \rangle \sim 20\ \mathrm{meV}$$

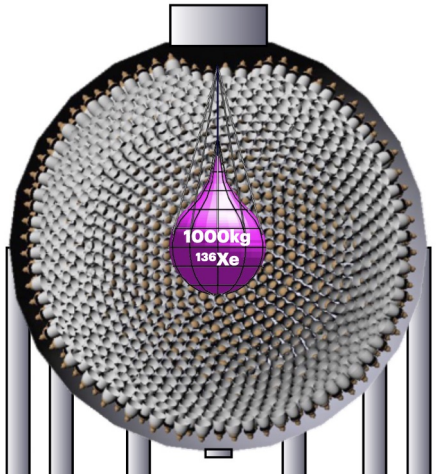

Towards the bottom of the IO region

Most promising isotope candidates: ^{76}Ge | ^{82}Se | ^{100}Mo | ^{130}Te | ^{136}Xe

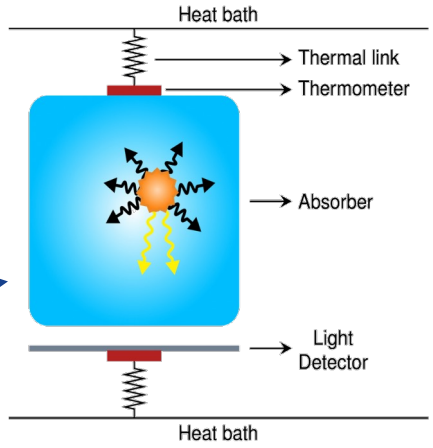

Examples of running experiments:

- ➢ CUORE: ^{130}Te Bolometer
- ➢ EXO-200: ^{136}Xe TPC
- ➢ LEGEND-200: ^{76}Ge semiconductor
- ➢ SNO+: ^{130}Te doped LS

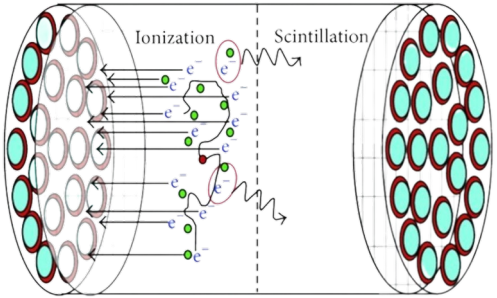

Next-generation ton-scale experiments:

CUPID ^{100}Mo bolometer | LEGEND-1000 | nEXO TPC 5ton 90% ^{136}Xe

Agostini, Matteo, et al. Rev. Mod. Phys. 95, 025002 (2023)

Possible detector locations and muon flux

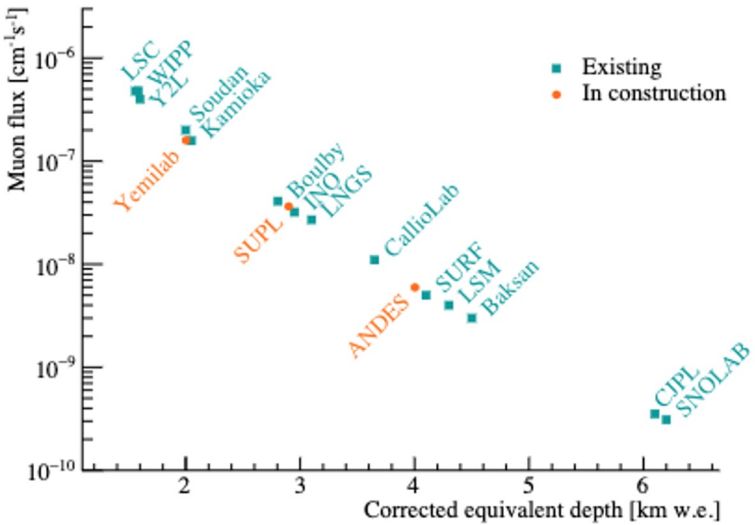

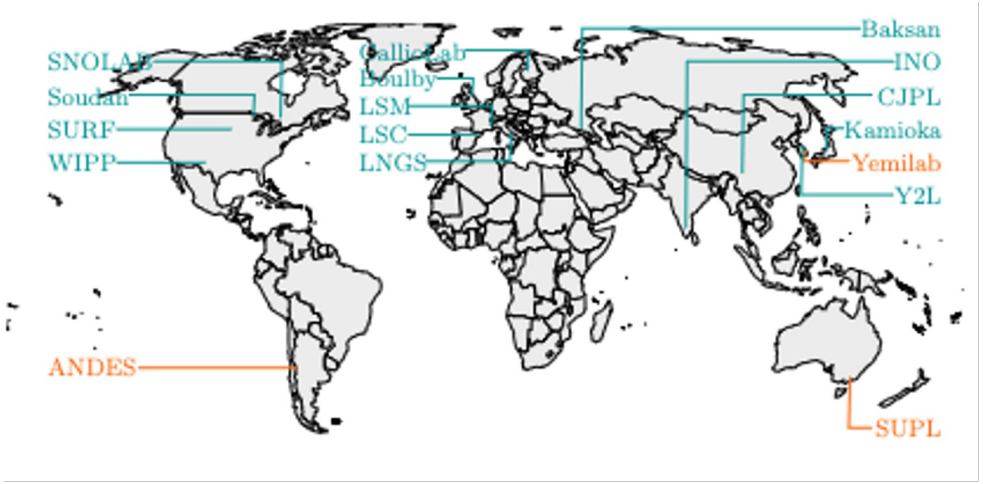

Agostini, Matteo, et al. Rev. Mod. Phys. 95, 025002 (2023)

$0\nu\beta\beta$ detectors and laboratory specifications

Laboratory	Country	Experiment(s)	Access	Depth (m.w.e)
Laboratoire Souterrain de Modane (LSM)	France	CUPID-Mo, SuperNEMO	Horizontal	4,800
Laboratorio Subterraneo de Canfranc (LSC)	Spain	NEXT-WHITE, NEXT-100, NEXT-HD module 1	Horizontal	2450
Yangyang Underground Laboratory	South Korea	AMoRE	Horizontal	2000
Kamioka Observatory	Japan	KamLAND-Zen, KamLAND2-Zen, CANDLES	Horizontal	2700
China Jinping Underground Laboratory (CJPL)	China	PandaX-III	Horizontal	6700
Sudbury Neutrino Observatory (SNOLAB)	Canada	SNO+, nEXO, LEGEND-1000	Vertical	6010
Sanford Underground Research Facility (SURF)	USA	Majorana Demonstrator, Theia	Vertical	4300
Gran Sasso National Laboratory (LNGS)	Italy	CUORE, CUPID, GERDA, LEGEND-200, LEGEND-1000	Horizontal	3400
Waste Isolation Pilot Plant (WIPP)*	USA	EXO-200	Vertical	2000

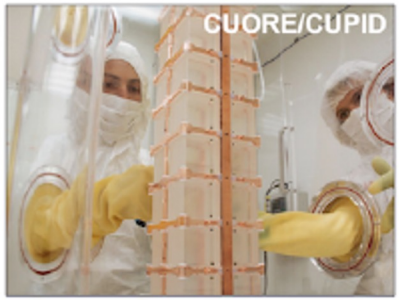

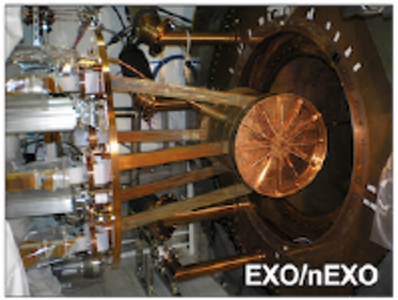

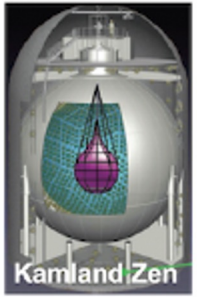

Radioactive and Solar Backgrounds

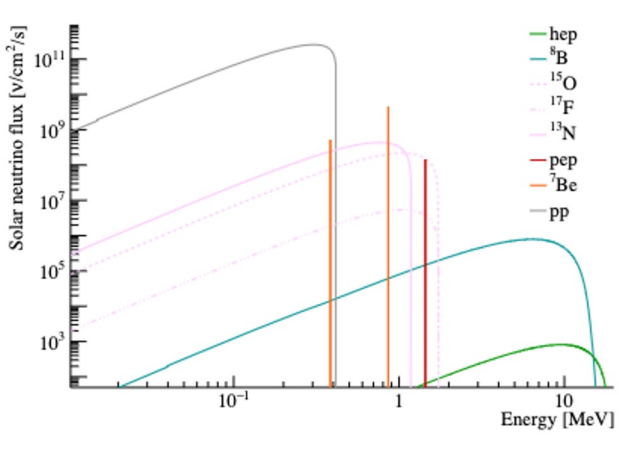

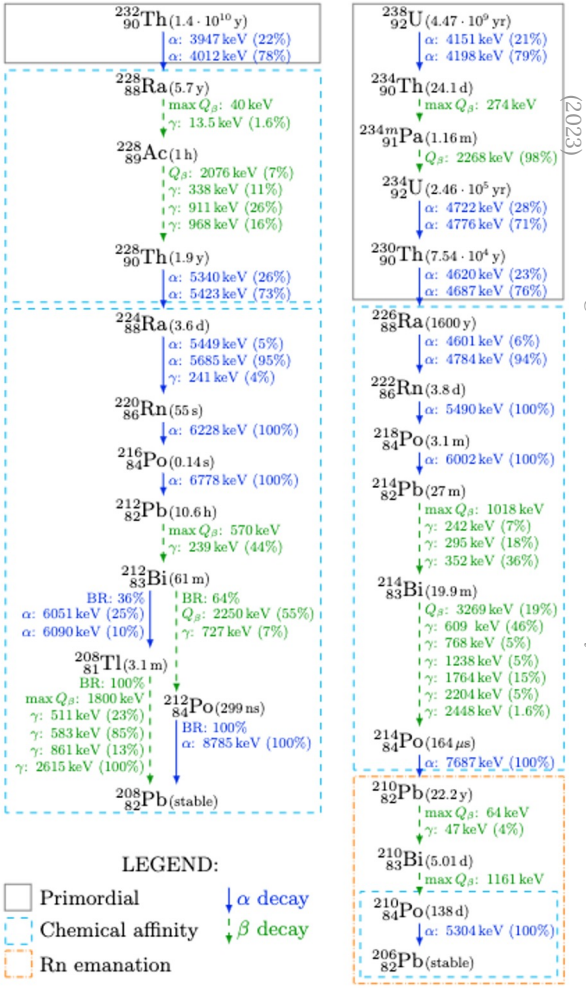

Agostini, Matteo, et al. Rev. Mod. Phys. 95, 025002 (2023)

$0\nu\beta\beta$ detector limits

Adams, C., et al. "Neutrinoless Double Beta Decay." arXiv preprint arXiv:2212.11099 (2022).

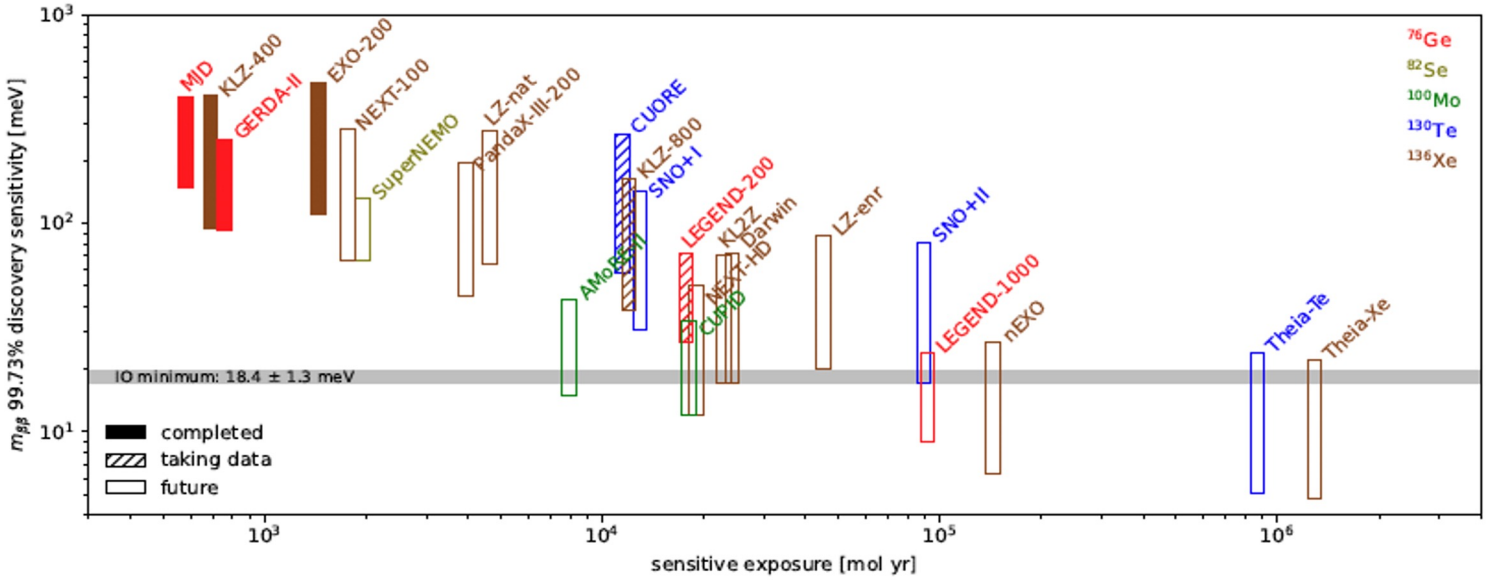

$0\nu\beta\beta$ detector limits

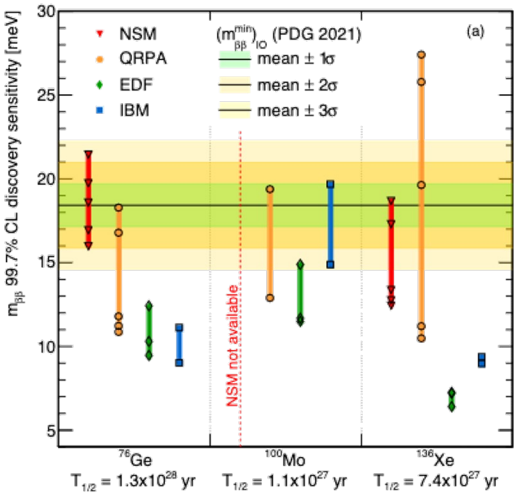

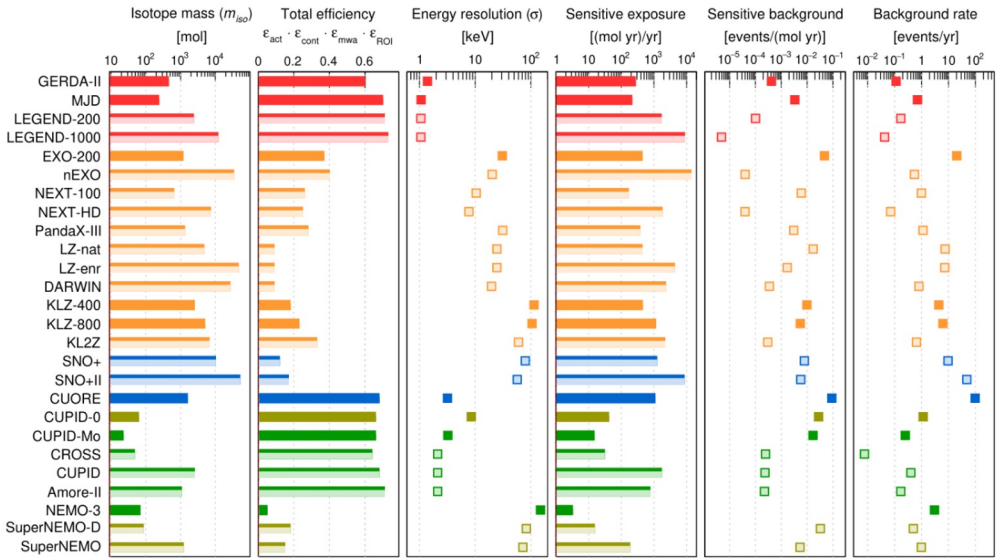

FIG. 20 Fundamental parameters driving the sensitive background and exposure, and consequently the sensitivity, of recent and future phases of existing experiments (see Eq. 47). Red bars are used for ^{76}Ge experiments, orange for ^{136}Xe, blue for ^{130}Te, green for ^{100}Mo, and sepia for ^{82}Se. Similar exposures are achieved with high mass but poorer energy resolution and efficiency by gas and liquid detectors, or with small mass but high resolution and efficiency by solid state detectors. The sensitive exposure is computed for one year of livetime. Ligher shades indicate experiments which are under construction or proposed.

54 (2023)

Agostini, Matteo, et al. Rev. Mod. Phys. 95, 025002

^{76}Ge
^{136}Xe
^{130}Te
^{100}Mo
^{82}Se

Future and current detector limits

Experiment	Isotope	Sensitivity limit (90% CL)		Exposure time	Reference
		$T^{0\nu}_{1/2}$ [year]	$m_{\beta\beta}$ [meV]	[year]	
DARWIN (baseline)	^{136}Xe	2.4×10^{27}	18–46	10	this work
DARWIN (ν dominated)	^{136}Xe	6.2×10^{27}	11–28	10	this work
KamLAND2-Zen	^{136}Xe	6×10^{26}	37–91	5	[37]
PandaX-III	^{136}Xe	1×10^{27}	28–71	3	[9]
NEXT-HD	^{136}Xe	3×10^{27}	16–41	10	[8]
nEXO	^{136}Xe	9.2×10^{27}	9–23	10	[10]
SNO+-II	^{130}Te	7×10^{26}	20–70	5	[37]
AMoRE-II	^{100}Mo	5×10^{26}	15–30	5	[37]
CUPID	^{130}Te / ^{100}Mo	$(2–5)\times10^{27}$	6-17	10	[37]
LEGEND-1000	^{76}Ge	1×10^{28}	11-28	10	[37]

Isotope	Technique	$T^{0\nu}_{1/2}$	$m_{\beta\beta}$ (eV)	Year Published
^{48}Ca	CaF_2 scint. crystals	$> 5.8 \times 10^{22}$ y	<3.5-22	2008 [65]
^{76}Ge	^{76}Ge detectors	$> 1.8 \times 10^{26}$ y	<0.079-0.180	2020 [12]
^{82}Se	$Zn^{82}Se$ bolometers	$> 4.6 \times 10^{24}$ y	<0.263-0.545	2022 [19]
^{96}Zr	Thin metal foil within TPC	$> 9.2 \times 10^{21}$ y	<3.9 - 19.5	2009 [66]
^{100}Mo	$Li_2{}^{100}MoO_4$ bolometers	$> 1.8 \times 10^{24}$ y	<0.28-0.49	2022 [18]
^{116}Cd	$^{116}CdWO_4$ scint. crystals	$> 2.2 \times 10^{23}$ y	<1.0-1.7	2018 [67]
^{128}Te	TeO_2 bolometers	$> 3.6 \times 10^{24}$ y	<1.5-4.0	2022 [68]
^{130}Te	TeO_2 bolometers	$> 2.2 \times 10^{25}$ y	<0.090-0.305	2022 [69]
^{136}Xe	Liquid Xe scintillators	$> 2.3 \times 10^{26}$ y	<0.036-0.156	2022 [13]
^{150}Nd	Thin metal foil within TPC	$> 2 \times 10^{22}$ y	1.6-5.3	2016 [70]

Sensitive background and exposure for recent and future experiments

FIG. 21 Sensitive background and exposure for recent and future experiments. The grey dashed lines indicate specific discovery sensitivity values on the $0\nu\beta\beta$-decay half-life. The colored dashed line indicate the half-life sensitivities required to test the bottom of the inverted ordering scenario for ^{76}Ge, ^{136}Xe, ^{130}Te ^{100}Mo, and ^{82}Se, assuming for each isotope the largest NME value among the QRPA calculations listed in Tab. I. A livetime of 10 yr is assumed except for completed experiments, for which the final reported exposure is used.

^{76}Ge
^{136}Xe
^{130}Te
^{100}Mo
^{82}Se

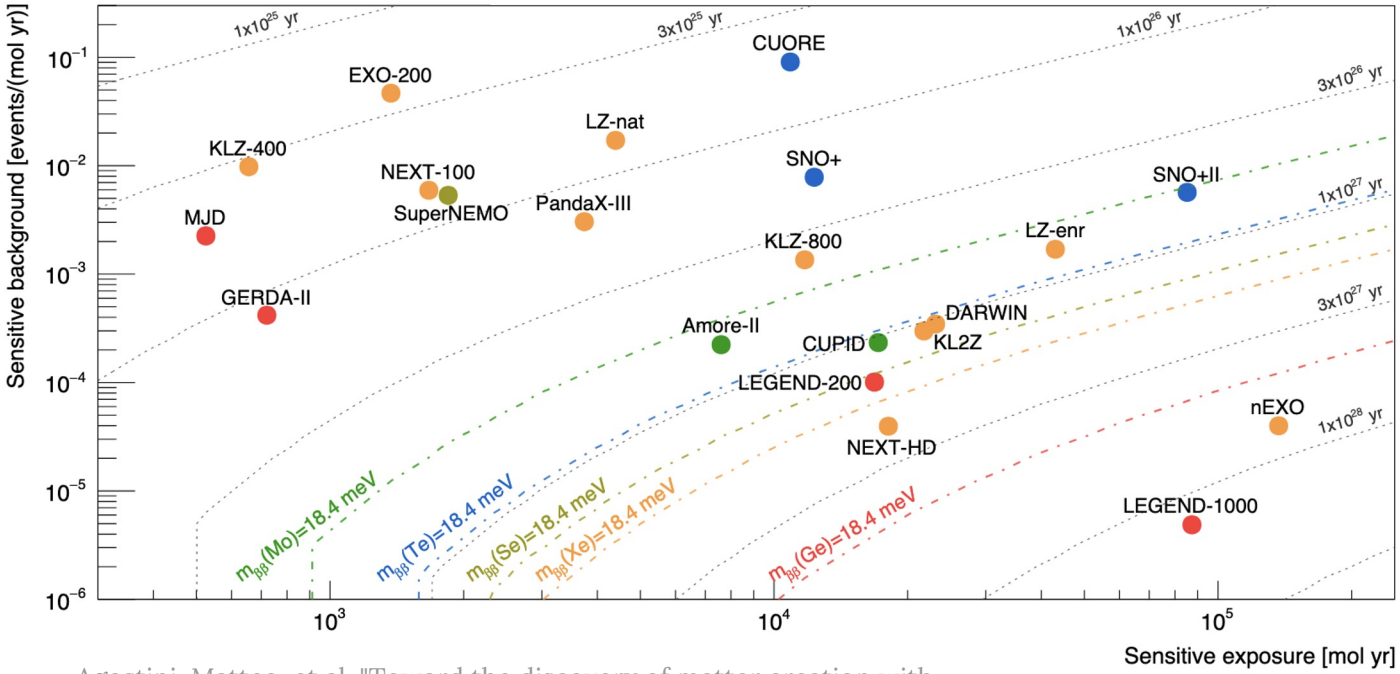

Agostini, Matteo, et al. Rev. Mod. Phys. 95, 025002 (2023)

Agostini, Matteo, et al. "Toward the discovery of matter creation with neutrinoless double-beta decay." *arXiv preprint arXiv*:2202.01787 (2022)

KamLAND-Zen background visualisation at IB region

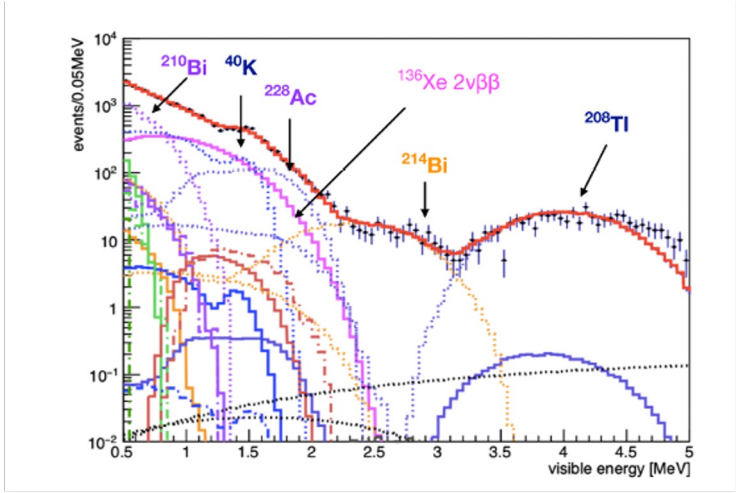

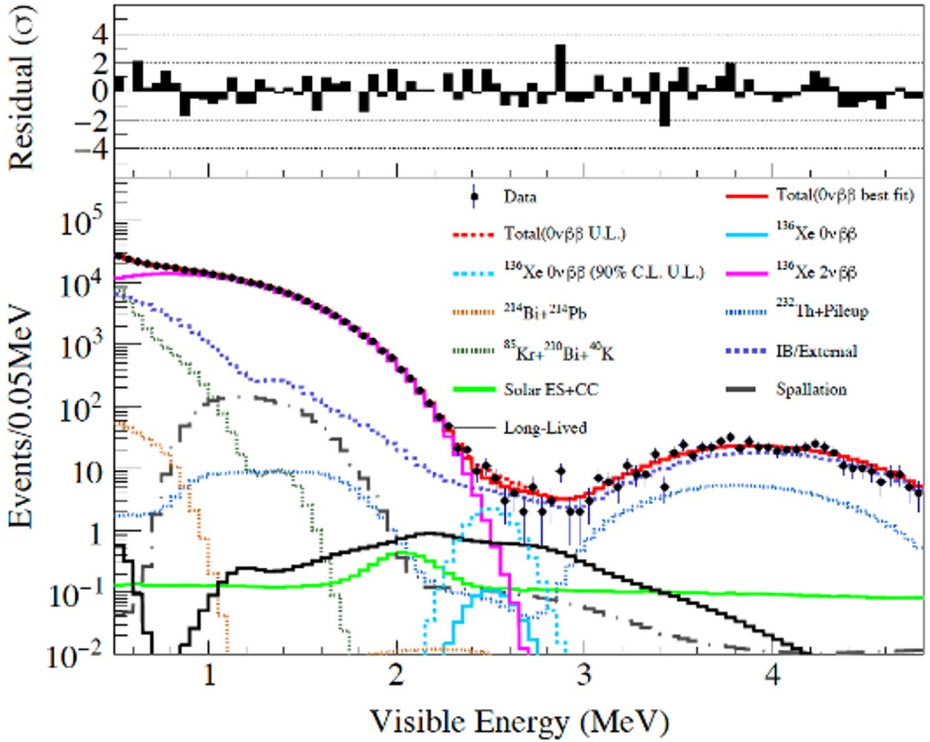

KamLAND-Zen data visualization

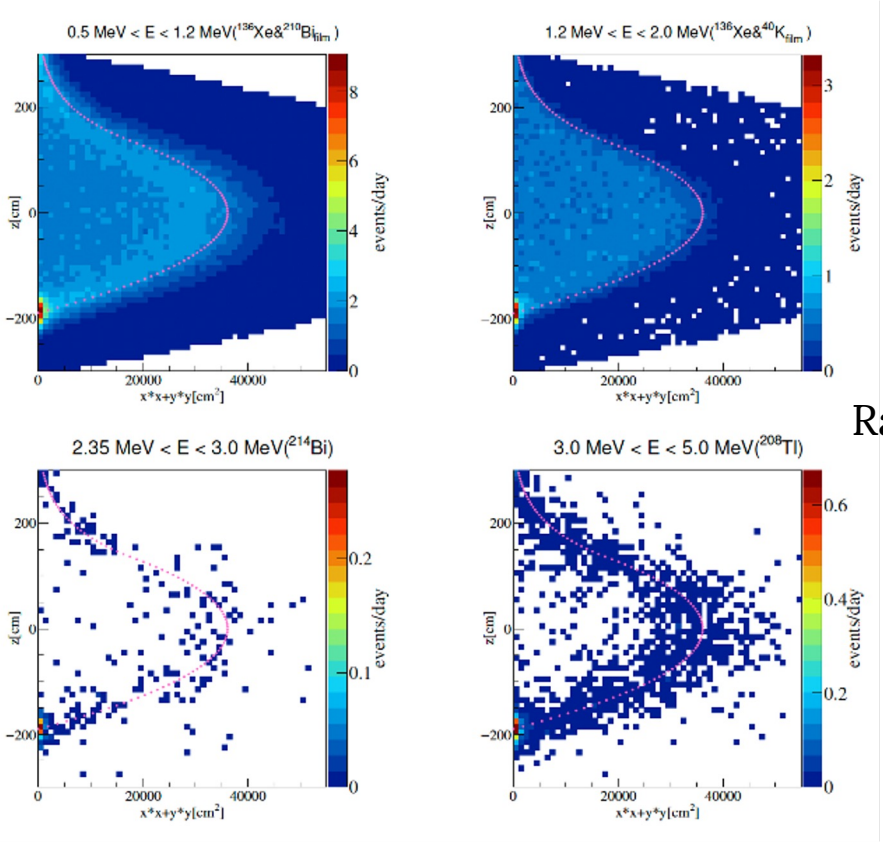

Rate dominated by 2vbb in 1.0 < E < 2.3

Which isotope is the best choice for detecting $0\nu\beta\beta$

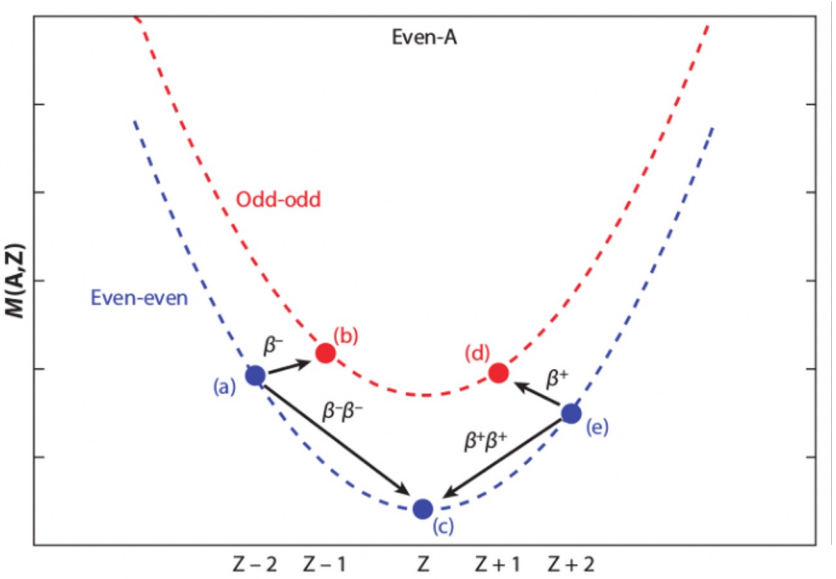

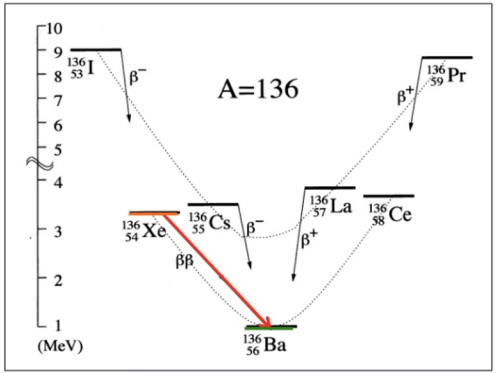

Natural abundance

Energy of peak

Phase space factor

Isotope	$G^{0\nu}$ (10^{-14} y^{-1})	$Q_{\beta\beta}$ (keV)	Nat. ab. (%)
^{48}Ca	6.35	4273.7	0.187
^{76}Ge	0.623	2039.1	7.8
^{82}Se	2.70	2995.5	9.2
^{96}Zr	5.63	3347.7	2.8
^{100}Mo	4.36	3035.0	9.6
^{110}Pd	1.40	2004.0	11.8
^{116}Cd	4.62	2809.1	7.6
^{124}Sn	2.55	2287.7	5.6
^{130}Te	4.09	2530.3	34.5
^{136}Xe	4.31	2461.9	8.9
^{150}Nd	19.2	3367.3	5.6

Other isotopes and muon spallation products

Table 4: Relevant parameters and features of the "magnificent nine" double-beta decay candidates.

Double-beta candidate	Q-value (MeV)	Phase space G_{01} (y^{-1})	Isotopic abundance (%)	Enrichable by centrifugation	Indicative cost normalized to Ge
^{48}Ca	4.27226 (404)	6.05×10^{-14}	0.187	No	—
^{76}Ge	2.03904 (16)	5.77×10^{-15}	7.8	Yes	1
^{82}Se	2.99512 (201)	2.48×10^{-14}	9.2	Yes	1
^{96}Zr	3.35037 (289)	5.02×10^{-14}	2.8	No	—
^{100}Mo	3.03440 (17)	3.89×10^{-14}	9.6	Yes	1
^{116}Cd	2.81350 (13)	4.08×10^{-14}	7.5	Yes	3
^{130}Te	2.52697 (23)	3.47×10^{-14}	33.8	Yes	0.2
^{136}Xe	2.45783 (37)	3.56×10^{-14}	8.9	Yes	0.1
^{150}Nd	3.37138 (20)	1.54×10^{-13}	5.6	No	—

Table 1 The most experimentally feasible isotopes and their key features

Isotope	Abundance (%)	$Q_{\beta\beta}$ (MeV)	$G^{2\nu}$ (10^{-18} year^{-1})
^{48}Ca	0.187	4.263	15.6
^{76}Ge	7.8	2.039	0.0482
^{82}Se	9.2	2.998	1.60
^{96}Zr	2.8	3.348	7.83
^{100}Mo	9.6	3.035	4.13
^{116}Cd	7.6	2.813	3.18
^{130}Te	34.08	2.527	1.53
^{136}Xe	8.9	2.459	1.43
^{150}Nd	5.6	3.371	36.4

The phase-space factors $G^{2\nu}$ are from Reference 4. $G^{2\nu}$ for ^{96}Zr, ^{100}Mo, and ^{116}Cd are calculated within the single-state dominance model (see Section 3).

Isotope	Half-life (s)	Decay mode	Yield (total) ($\times 10^{-7}\mu^{-1}g^{-1}cm^2$)	Yield ($E > 3.5$ MeV) ($\times 10^{-7}\mu^{-1}g^{-1}cm^2$)	Primary process
n			2030		
^{18}N	0.624	β^-	0.02	0.01	^{18}O(n,p)
^{17}N	4.173	$\beta^- n$	0.59	0.02	^{18}O$(n,n+p)$
^{16}N	7.13	$\beta^-\gamma$ (66%), β^- (28%)	18	18	(n,p)
^{16}C	0.747	$\beta^- n$	0.02	0.003	$(\pi^- n+p)$
^{15}C	2.449	$\beta^-\gamma$ (63%), β^- (37%)	0.82	0.28	$(n,2p)$
^{14}B	0.0138	$\beta^-\gamma$	0.02	0.02	$(n,3p)$
^{13}O	0.0086	β^+	0.26	0.24	$(\mu^-,p+2n+\mu^-+\pi^-)$
^{13}B	0.0174	β^-	1.9	1.6	$(\pi^-,2p+n)$
^{12}N	0.0110	β^+	1.3	1.1	$(\pi^+,2p+2n)$
^{12}B	0.0202	β^-	12	9.8	$(n,\alpha+p)$
^{12}Be	0.0236	β^-	0.10	0.08	$(\pi^-,\alpha+p+n)$
^{11}Be	13.8	β^- (55%), $\beta^-\gamma$ (31%)	0.81	0.54	$(n,\alpha+2p)$
^{11}Li	0.0085	$\beta^- n$	0.01	0.01	$(\pi^+,5p+\pi^++\pi^0)$
^{9}C	0.127	β^+	0.89	0.69	$(n,\alpha+4n)$
^{9}Li	0.178	$\beta^- n$ (51%), β^- (49%)	1.9	1.5	$(\pi^-,\alpha+2p+n)$
^{8}B	0.77	β^+	5.8	5.0	$(\pi^+,\alpha+2p+2n)$
^{8}Li	0.838	β^-	13	11	$(\pi^-,\alpha+{}^2H+p+n)$
^{8}He	0.119	$\beta^-\gamma$ (84%), $\beta^- n$ (16%)	0.23	0.16	$(\pi^-,{}^3H+4p+n)$
^{15}O			351		(γ,n)
^{15}N			773		(γ,p)
^{14}O			13		$(n,3n)$
^{14}N			295		$(\gamma,n+p)$
^{14}C			64		$(n,n+2p)$
^{13}N			19		$(\gamma,{}^3H)$
^{13}C			225		$(n,{}^2H+p+n)$
^{12}C			792		(γ,α)
^{11}C			105		$(n,\alpha+2n)$
^{11}B			174		$(n,\alpha+p+n)$
^{10}C			7.6		$(n,\alpha+3n)$
^{10}B			77		$(n,\alpha+p+2n)$
^{10}Be			24		$(n,\alpha+2p+n)$
^{9}Be			38		$(n,2\alpha)$
sum			3015	50	

Xenon spallation FLUKA simulations

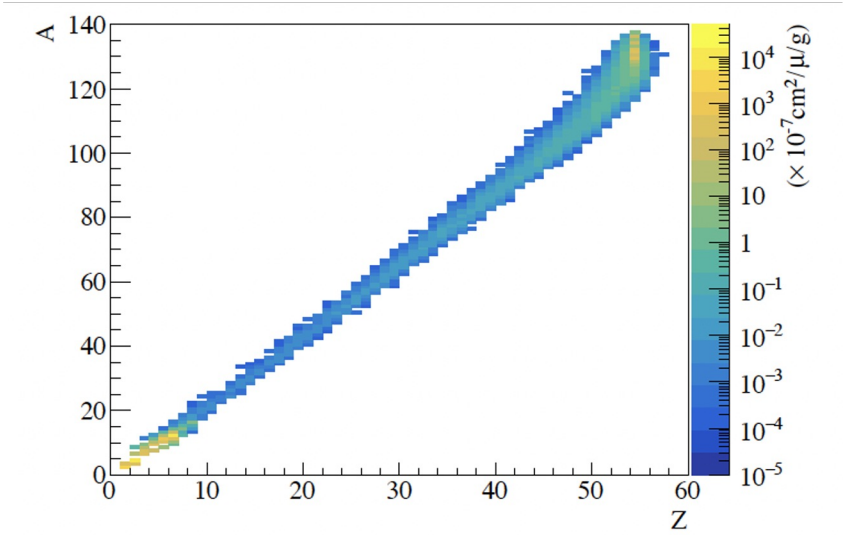

TABLE IX. Simulated production rate of dominant isotopes in $2.35 \leq E \leq 2.70$ MeV in Xe-LS.

	$\tau_{1/2}$ (s)	Q (MeV)	(kton day)$^{-1}$ ROI	Total
^{88}Y	9.212×10^6	3.62 (EC/$\beta^+\gamma$)	0.110	0.136
^{90m1}Zr	8.092×10^{-1}	2.31 (IT)	0.012	0.093
^{90}Nb	5.256×10^4	6.11 (EC/$\beta^+\gamma$)	0.024	0.095
^{96}Tc	3.698×10^5	2.97 (EC/$\beta^+\gamma$)	0.012	0.059
^{98}Rh	5.232×10^2	5.06 (EC/$\beta^+\gamma$)	0.011	0.076
^{100}Rh	7.488×10^4	3.63 (EC/$\beta^+\gamma$)	0.088	0.234
^{104}Ag	4.152×10^3	4.28 (EC/$\beta^+\gamma$)	0.012	0.160
^{104m1}Ag	2.010×10^3	4.28 (EC/$\beta^+\gamma$)	0.018	0.111
^{107}In	1.944×10^3	3.43 (EC/$\beta^+\gamma$)	0.019	0.135
^{108}In	3.480×10^3	5.16 (EC/$\beta^+\gamma$)	0.089	0.194
^{110}In	1.771×10^4	3.89 (EC/$\beta^+\gamma$)	0.053	0.236
^{110m1}In	4.146×10^3	3.89 (EC/$\beta^+\gamma$)	0.066	0.351
^{109}Sn	1.080×10^3	3.85 (EC/$\beta^+\gamma$)	0.027	0.122
^{113}Sb	4.002×10^2	3.92 (EC/$\beta^+\gamma$)	0.036	0.231
^{114}Sb	2.094×10^2	5.88 (EC/$\beta^+\gamma$)	0.020	0.297
^{115}Sb	1.926×10^3	3.03 (EC/$\beta^+\gamma$)	0.031	0.839
^{116}Sb	9.480×10^2	4.71 (EC/$\beta^+\gamma$)	0.071	0.939
^{118}Sb	2.160×10^2	3.66 (EC/$\beta^+\gamma$)	0.165	1.288
^{124}Sb	5.201×10^6	2.90 (EC/$\beta^-\gamma$)	0.016	0.054
^{115}Te	3.480×10^2	4.64 (EC/$\beta^+\gamma$)	0.012	0.124
^{117}Te	3.720×10^3	3.54 (EC/$\beta^+\gamma$)	0.052	0.594
^{119}I	1.146×10^3	3.51 (EC/$\beta^+\gamma$)	0.053	0.533
^{120}I	4.896×10^3	5.62 (EC/$\beta^+\gamma$)	0.091	0.953
^{122}I	2.178×10^2	4.23 (EC/$\beta^+\gamma$)	0.289	1.965
^{124}I	3.608×10^5	3.16 (EC/$\beta^+\gamma$)	0.190	1.654
^{130}I	4.450×10^4	2.95 ($\beta^-\gamma$)	0.195	1.188
^{132}I	8.262×10^3	3.58 ($\beta^-\gamma$)	0.148	0.427
^{134}I	3.150×10^3	4.18 ($\beta^-\gamma$)	0.043	0.183
^{121}Xe	2.406×10^3	3.75 (EC/$\beta^+\gamma$)	0.100	0.540
^{125}Cs	2.802×10^3	3.09 (EC/$\beta^+\gamma$)	0.012	0.266
^{126}Cs	9.840×10^1	4.82 (EC/$\beta^+\gamma$)	0.011	0.080
^{128}Cs	2.196×10^2	3.93 (EC/$\beta^+\gamma$)	0.031	0.229

High energetic muons flying through the detector

Muon track reconstruction and induced showers

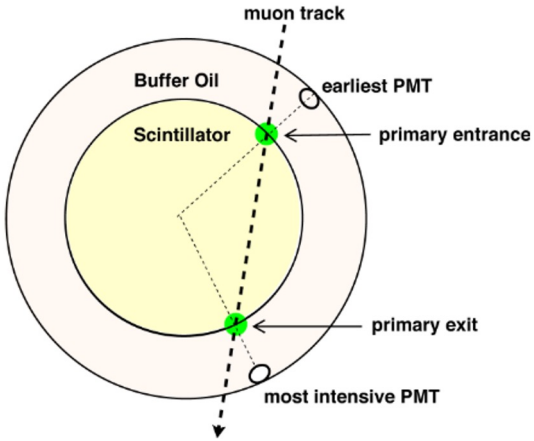

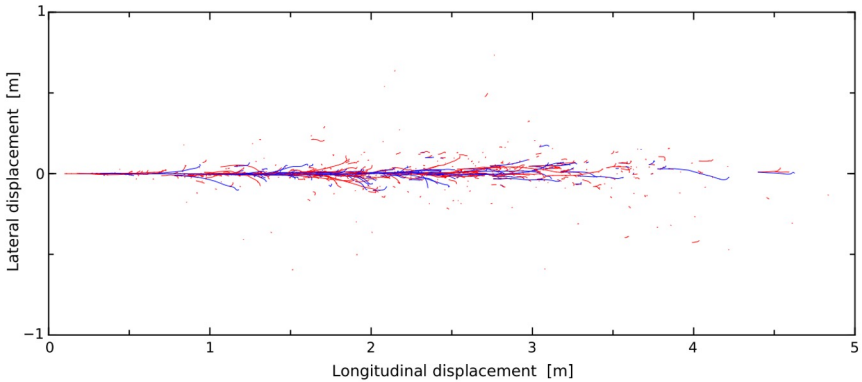

O. Hideyoshi, High Sensitivity Search for Neutrinoless Double-Beta Decay in KamLAND-Zen with Double Amount of 136Xe. PhD thesis, Tohoku University, 2020.

S. W. Li and J. F. Beacom, "Spallation backgrounds in super-kamiokande are made in muon-induced showers," *Physical Review D*, vol. 91, no. 10, p. 105005, 2015

High energetic muons flying through the detector

Triple coincidence tagging of muon spallation products

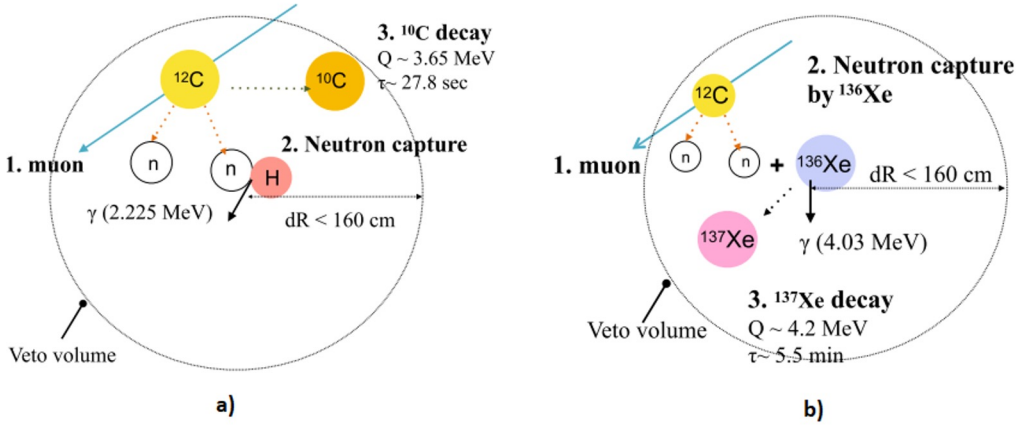

O. Hideyoshi, High Sensitivity Search for Neutrinoless Double-Beta Decay in KamLAND-Zen with Double Amount of 136Xe. PhD thesis, Tohoku University, 2020.

TABLE IV Fundamental parameters driving the sensitive background and exposure of recent and future phases of existing experiments. The last two columns report the discovery sensitivity on the $0\nu\beta\beta$-decay half-life for 10 years of livetime, and the corresponding sensitivity on $m_{\beta\beta}$ for the range of NMEs specified in Tab. I. For completed experiments, sensitivities are computed using the reported final exposure. MJD, KLZ, and SuperNEMO-D refer to the MAJORANA DEMONSTRATOR, KamLAND-Zen, and the SuperNEMO Demonstrator, respectively.

Experiment	Isotope	Status	Lab	$m_{\rm iso}$ [mol]	$\varepsilon_{\rm act}$ [%]	$\varepsilon_{\rm cont}$ [%]	$\varepsilon_{\rm mva}$ [%]	σ [keV]	ROI [σ]	$\varepsilon_{\rm ROI}$ [%]	$\mathcal{E}$ $\left[\frac{\rm mol\cdot yr}{yr}\right]$	$\mathcal{B}$ $\left[\frac{\rm events}{\rm mol\cdot yr}\right]$	λ_b $\left[\frac{\rm events}{\rm yr}\right]$	$T_{1/2}$ [yr]	$m_{\beta\beta}$ [meV]
High-purity Ge detectors (Sec. VI.B)															
GERDA-II	^{76}Ge	completed	LNGS	$4.5\cdot10^{2}$	88	91	79	1.4	-2,2	95	273	$4.2\cdot10^{-4}$	$1.1\cdot10^{-1}$	$1.2\cdot10^{26}$	93-222
MJD	^{76}Ge	completed	SURF	$3.1\cdot10^{2}$	91	91	86	1.1	-2,2	95	212	$3.3\cdot10^{-3}$	$7.1\cdot10^{-1}$	$4.7\cdot10^{25}$	149-355
LEGEND-200	^{76}Ge	construction	LNGS	$2.4\cdot10^{3}$	91	91	90	1.1	-2,2	95	1 684	$1.0\cdot10^{-4}$	$1.7\cdot10^{-1}$	$1.5\cdot10^{27}$	27-63
LEGEND-1000	^{76}Ge	proposed		$1.2\cdot10^{4}$	92	92	90	1.1	-2,2	95	8 736	$4.9\cdot10^{-6}$	$4.3\cdot10^{-2}$	$1.3\cdot10^{28}$	9-21
Xenon time projection chambers (Sec. VI.C)															
EXO-200	^{136}Xe	completed	WIPP	$1.2\cdot10^{3}$	46	100	84	31	-2,2	95	438	$4.7\cdot10^{-2}$	$2.1\cdot10^{+1}$	$2.4\cdot10^{25}$	111-477
nEXO	^{136}Xe	proposed	SNOLAB	$3.4\cdot10^{4}$	64	100	66	20	-2,2	95	13 700	$4.0\cdot10^{-5}$	$5.5\cdot10^{-1}$	$7.4\cdot10^{27}$	6-27
NEXT-100	^{136}Xe	construction	LSC	$6.4\cdot10^{2}$	88	76	49	10	-1.0,1.8	80	167	$5.9\cdot10^{-3}$	$9.9\cdot10^{-1}$	$7.0\cdot10^{25}$	66-281
NEXT-HD	^{136}Xe	proposed		$7.4\cdot10^{3}$	95	89	44	7.7	-0.5,1.7	65	1 809	$4.0\cdot10^{-5}$	$7.2\cdot10^{-2}$	$2.2\cdot10^{27}$	12-50
PandaX-III-200	^{136}Xe	construction	CJPL	$1.3\cdot10^{3}$	77	74	65	31	-1.2,1.2	76	374	$3.0\cdot10^{-3}$	$1.1\cdot10^{+0}$	$1.5\cdot10^{26}$	45-194
LZ-nat	^{136}Xe	construction	SURF	$4.7\cdot10^{3}$	14	100	80	25	-1.4,1.4	84	440	$1.7\cdot10^{-2}$	$7.5\cdot10^{+0}$	$7.2\cdot10^{25}$	64-277
LZ-enr	^{136}Xe	proposed	SURF	$4.6\cdot10^{4}$	14	100	80	25	-1.4,1.4	84	4302	$1.7\cdot10^{-3}$	$7.3\cdot10^{+0}$	$7.1\cdot10^{26}$	20-87
Darwin	^{136}Xe	proposed		$2.7\cdot10^{4}$	13	100	90	20	-1.2,1.2	76	2 312	$3.5\cdot10^{-4}$	$8.0\cdot10^{-1}$	$1.1\cdot10^{27}$	17-72
Large liquid scintillators (Sec. VI.D)															
KLZ-400	^{136}Xe	completed	Kamioka	$2.5\cdot10^{3}$	44	100	97	114	0,1.4	42	450	$9.8\cdot10^{-3}$	$4.4\cdot10^{+0}$	$3.3\cdot10^{25}$	95-408
KLZ-800	^{136}Xe	taking data	Kamioka	$5.0\cdot10^{3}$	55	100	100	105	0,1.4	42	1 143	$5.5\cdot10^{-3}$	$6.2\cdot10^{+0}$	$2.0\cdot10^{26}$	38-164
KL2Z	^{136}Xe	proposed	Kamioka	$6.7\cdot10^{3}$	80	100	97	60	0,1.4	42	2 176	$3.0\cdot10^{-4}$	$6.5\cdot10^{-1}$	$1.1\cdot10^{27}$	17-71
SNO+I	^{130}Te	construction	SNOLAB	$1.0\cdot10^{4}$	20	100	97	80	-0.5,1.5	62	1 232	$7.8\cdot10^{-3}$	$9.7\cdot10^{+0}$	$1.8\cdot10^{26}$	31-144
SNO+II	^{130}Te	proposed	SNOLAB	$5.1\cdot10^{4}$	27	100	97	57	-0.5,1.5	62	8 521	$5.7\cdot10^{-3}$	$4.8\cdot10^{+1}$	$5.7\cdot10^{26}$	17-81
Cryogenic calorimeters (Sec. VI.E)															
CUORE	^{130}Te	taking data	LNGS	$1.6\cdot10^{3}$	100	88	92	3.2	-1.4,1.4	84	1 088	$9.1\cdot10^{-2}$	$9.9\cdot10^{+1}$	$5.1\cdot10^{25}$	58-270
CUPID-0	^{82}Se	completed	LNGS	$6.2\cdot10^{1}$	100	81	86	8.5	-2,2	95	41	$2.8\cdot10^{-2}$	$1.2\cdot10^{+0}$	$4.4\cdot10^{24}$	283-551
CUPID-Mo	^{100}Mo	completed	LSM	$2.3\cdot10^{1}$	100	76	91	3.2	-2,2	95	15	$1.7\cdot10^{-2}$	$2.5\cdot10^{-1}$	$1.7\cdot10^{24}$	293-858
CROSS	^{100}Mo	construction	LSC	$4.8\cdot10^{1}$	100	75	90	2.1	-2,2	95	31	$2.5\cdot10^{-4}$	$7.6\cdot10^{-3}$	$4.9\cdot10^{25}$	54-160
CUPID	^{100}Mo	proposed	LNGS	$2.5\cdot10^{3}$	100	79	90	2.1	-2,2	95	1 717	$2.3\cdot10^{-4}$	$4.0\cdot10^{-1}$	$1.1\cdot10^{27}$	12-34
AMoRE-II	^{100}Mo	proposed	Yemilab	$1.1\cdot10^{3}$	100	82	91	2.1	-2,2	95	760	$2.2\cdot10^{-4}$	$1.7\cdot10^{-1}$	$6.7\cdot10^{26}$	15-43
Tracking calorimeters (Sec. VI.F)															
NEMO-3	^{100}Mo	completed	LSM	$6.9\cdot10^{1}$	100	100	11	148	-1.6,1.1	42	3	$9.4\cdot10^{-1}$	$3.0\cdot10^{+0}$	$5.6\cdot10^{23}$	505-1485
SuperNEMO-D	^{82}Se	construction	LSM	$8.5\cdot10^{1}$	100	100	28	83	-4.2,2.4	64	15	$3.3\cdot10^{-2}$	$5.0\cdot10^{-1}$	$8.6\cdot10^{24}$	201-391
SuperNEMO	^{82}Se	proposed	LSM	$1.2\cdot10^{3}$	100	100	28	72	-4.1,2.8	54	185	$5.3\cdot10^{-3}$	$9.8\cdot10^{-1}$	$7.8\cdot10^{25}$	67-131

Agostini, Matteo, et al. Rev. Mod. Phys. 95, 025002 (2023)

Experiment	Isotope	Mass	Technique	Present Status	Location
CANDLES-III [124]	^{48}Ca	305 kg	$^{nat}CaF_2$ scint. crystals	Operating	Kamioka
CDEX-1 [125]	^{76}Ge	1 kg	^{enr}Ge semicond. det.	Prototype	CJPL
CDEX-300ν [125]	^{76}Ge	225 kg	^{enr}Ge semicond. det.	Construction	CJPL
LEGEND-200 [16]	^{76}Ge	200 kg	^{enr}Ge semicond. det.	Commissioning	LNGS
LEGEND-1000 [16]	^{76}Ge	1 ton	^{enr}Ge semicond. det.	Proposal	
CUPID-0 [19]	^{82}Se	10 kg	Zn^{enr}Se scint. bolometers	Prototype	LNGS
SuperNEMO-Dem [126]	^{82}Se	7 kg	^{enr}Se foils/tracking	Operation	Modane
SuperNEMO [126]	^{82}Se	100 kg	^{enr}Se foils/tracking	Proposal	Modane
Selena [127]	^{82}Se		^{enr}Se, CMOS	Development	
IFC [128]	^{82}Se		ion drift SeF_6 TPC	Development	
CUPID-Mo [17]	^{100}Mo	4 kg	Li$^{enr}MoO_4$,scint. bolom.	Prototype	LNGS
AMoRE-I [129]	^{100}Mo	6 kg	^{40}Ca$^{100}MoO_4$ bolometers	Operation	YangYang
AMoRE-II [129]	^{100}Mo	200 kg	^{40}Ca$^{100}MoO_4$ bolometers	Construction	Yemilab
CROSS [130]	^{100}Mo	5 kg	$Li_2{}^{100}MoO_4$, surf. coat bolom.	Prototype	Canfranc
BINGO [131]	^{100}Mo		Li$^{enr}MoO_4$	Development	LNGS
CUPID [28]	^{100}Mo	450 kg	Li$^{enr}MoO_4$,scint. bolom.	Proposal	LNGS
China-Europe [132]	^{116}Cd		$^{enr}CdWO_4$ scint. crystals	Development	CJPL
COBRA-XDEM [133]	^{116}Cd	0.32 kg	^{nat}Cd CZT semicond. det.	Operation	LNGS
Nano-Tracking [134]	^{116}Cd		^{nat}CdTe. det.	Development	
TIN.TIN [135]	^{124}Sn		Tin bolometers	Development	INO
CUORE [10]	^{130}Te	1 ton	TeO_2 bolometers	Operating	LNGS
SNO+ [136]	^{130}Te	3.9 t	0.5-3% ^{nat}Te loaded liq. scint.	Commissioning	SNOLab
nEXO [29]	^{136}Xe	5 t	Liq. ^{enr}Xe TPC/scint.	Proposal	
NEXT-100 [137]	^{136}Xe	100 kg	gas TPC	Construction	Canfranc
NEXT-HD [137]	^{136}Xe	1 ton	gas TPC	Proposal	Canfranc
AXEL [138]	^{136}Xe		gas TPC	Prototype	
KamLAND-Zen-800 [13]	^{136}Xe	745 kg	^{enr}Xe disolved in liq. scint.	Operating	Kamioka
KamLAND2-Zen [41]	^{136}Xe		^{enr}Xe disolved in liq. scint.	Development	Kamioka
LZ [139]	^{136}Xe	600 kg	Dual phase Xe TPC, nat./enr. Xe	Operation	SURF
PandaX-4T [119]	^{136}Xe	3.7 ton	Dual phase nat. Xe TPC	Operation	CJPL
XENONnT [140]	^{136}Xe	5.9 ton	Dual phase Xe TPC	Operating	LNGS
DARWIN [141]	^{136}Xe	50 ton	Dual phase Xe TPC	Proposal	LNGS
R2D2 [142]	^{136}Xe		Spherical Xe TPC	Development	
LAr TPC [143]	^{136}Xe	kton	Xe-doped LR TPC	Development	
NuDot [144]	Various		Cherenkov and scint. in liq. scint.	Development	
THEIA [145]	Xe or Te		Cherenkov and scint. in liq. scint.	Development	
JUNO [146]	Xe or Te		Doped liq. scint.	Development	
Slow-Fluor [147]	Xe or Te		Slow Fluor Scint.	Development	

Adams, C., et al. "Neutrinoless Double Beta Decay." arXiv preprint arXiv:2212.11099 (2022).

Experimental design criteria for $0\nu\beta\beta$

Direct searches: kinematic parameters of the two electrons

➔ Total energy and individual electron paths

$$T^{0\nu}_{1/2} = \ln 2 \frac{N_A}{W} \left(\frac{a \cdot \epsilon \cdot M}{N_{\text{obs}}} \right) t \quad \propto \begin{cases} a\epsilon \cdot Mt \\ a\epsilon \sqrt{\dfrac{Mt}{N_{\text{bkg}} \cdot \Delta E}} \end{cases}$$

Detector and isotope choice depending on:

- High isotopic abundance — a
- Deployment in large quantity — M
- High-resolution detector — ΔE
- Low-background conditions — N_{bkg}